Temperature induced tissue deformation monitored by dynamic speckle interferometry

K. Bliedtner, E. Seifert, and R. Brinkmann

***Abstract*—Photocoagulation is a common retinal laser treatment. Intra- and inter-individual variations of light scattering and absorption conditions make it impossible to achieve lesions of equal strength without a real-time temperature control. An optical temperature control concept may be based on laser speckle analysis, which is investigated in this work.**

A HeNe laser (633nm) was used for illumination of the porcine RPE and RPE models heated by a standard coagulation laser (532nm) using different irradiances. The scattered light was imaged on a CCD camera and then analyzed regarding speckle movement.

It could be demonstrated that the speckle movement is radial towards the center of heating and accordingly reverse during relaxation. Furthermore a correlation between the magnitude of movement and the irradiance could be shown.

I. Introduction

Photocoagulation is a laser therapy for a variety of retinal diseases. It has become a clinical standard treatment for diabetic retinopathy, branch vein occlusion and central retinal vein occlusion [1]–[4]. During photocoagulation the laser light is absorbed by pigmented structures (mainly the retinal pigment epithelium (RPE)) which is consequently heated. Thermal denaturation along with cell apoptosis or necrosis follows a sufficient heating. This technique is used for instance to suppress the detachment of the retina through artificial scar production or the coagulation of peripheral photoreceptors to improve the hemodynamics and the oxygenation of the macula and hereby reduce neovascularisation [2]. The laser parameter settings vary according to the disease however for retinal photocoagulation laser power from 50 to 500 mW is applied for an irradiation time of 20 to 200 ms onto a spot diameter ranging over 50 to 500 µm [2]–[4].

Constant laser parameters may lead to different heat development and undesirable thermal damage because of strong variations of pigmentation not only in the RPE and the choroid between different patient but also because of a local alteration within the RPE [5], [6]. The light scattering properties of the anterior eye media varying with age and disease intensify this effect. Also the risk of choroidal rupture and bleeding caused by excessive lesions which increases the pain for the patient can not be underrated. The only control for successful treatment is an subjective evaluation of visible whitening of the lesion caused by the increased scattering after denaturation which may take a whole day to fully develop [7]. The laser power can be increased for each spot until the whitening appears, which is not feasible during one treatment session regarding the overall heating time for up to several hundred lesions. To achieve uniform lesions and avoid unnecessary strong damage an objective real time temperature monitoring is required to regulate exposure time and power via induced temperature increase.

A non-invasive feedback system, already tested on rabbits, is based on optoacoustic waves evoked by thermoelastic expansion of the tissue due to heating. Additionally to the laser irradiation nanosecond laser pulses are applied to evoke temperature dependent pressure waves which are detected by an ultrasonic transducer included in a contact lens. The temperature can then be measured indirectly by the increase of the amplitude of the optoacoustic signal due to temperature dependence of the material specific Grüneisen parameter [8]. The main disadvantage is the dependence of the optoacoustic transients on the position of the treated loaction, the inability to measure temperatures above 60°C and the rather complex setup.

Temperature induced tissue movements could be a reasonable signal source for such a temperature control system. Techniques based on the analysis of random interference patterns (laser speckle) are sensitive to in-plane and out of-plane displacements of the tissue. In order to choose a proper laser speckle technique the kind of speckle movements needs to be known. In this project a signal characterization of dynamic speckles has been carried out using speckle photography techniques.

II. Material and Methods

A. Dynamic Laser Speckle

The basic idea is that if a rough surface is illuminated with coherent laser light the backscattered light will form a random pattern with alternating bright and dark spots of various intensity and shape, the so called speckle pattern, caused by the interference of multiple scattered wavelets with a random amplitude and phase [9]. When the object or parts of it are moving the pattern is altering as well. Those dynamic speckle can usually be divided in two groups, translational speckle and boiling speckle. Translational speckle remain unchanged in their shape and the whole grain is moving with a movement of the diffuser. Boiling speckle change in size, disappear and reappear without a significant variation of their position [9]. The following section describes the capture and determines the dynamics of speckle produced by the thermal expansion and relaxation of the tissue due to heating during photocoagulation.

K. Bliedtner, Medizinische Ingenieurwissenschaft, University of Luebeck; the work has been carried out at the Institute of Biomedical Optics, University of Luebeck, Luebeck, Germany (e-mail: bliedtne@miw.uni-luebeck.de).

E. Seifert is with the Medical Laser Center Luebeck GmbH, Luebeck, Germany (e-mail: eric.seifert@mll.uni-luebeck.de).

R. Brinkmann is with the Medical Laser Center Luebeck, Luebeck Germany and the Institute of Biomedical Optics, University of Luebeck, Luebeck, Germany (e-mail: brinkmann@bmo.uni-luebeck.de).

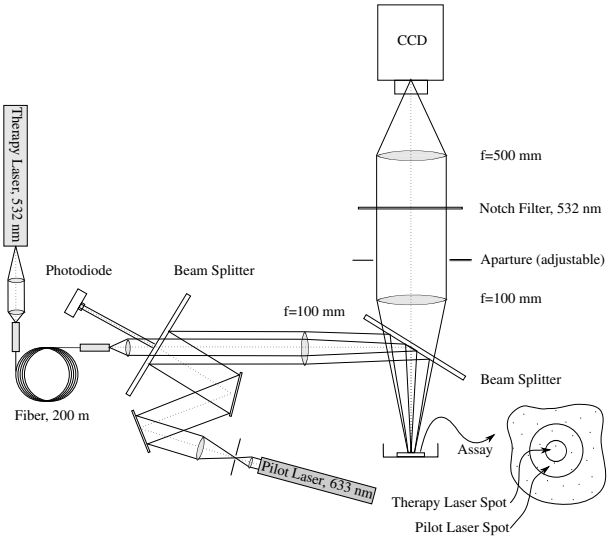

Fig. 1: Optical setup: heating and pilot laser are superimposed and focused on the assay. The scattered light is captured via optics by the CCD camera.

B. Optical Setup

For heating a frequency doubled solid state laser at 532 nm (Visulas 532s, Carl Zeiss) is launched in a 200 m long fiber for a sufficient beam quality. Because of the different path lengths of the modes passing through the fiber, they are interfering which causes a certain intensity distribution at the end of the fiber. The longer the fiber the more mixing of energy between the modes propagating through the fiber occurs and hence a more homogeneous intensity profile can be obtained, which is requested for a homogeneous heating over the whole spot area. Inhomogeneous spots with intensity peaks can lead to strong heating in small areas and may lead to irregular thermal expansion and thus to chaotic speckle movement.

Fig. 2A shows the speckle pattern (captured with a beam profiler, Data Ray Inc., WinCamD-XHR) of a standard coagulation laser fiber (fiber A) with a length of 2 m, a core diameter of 50 µm and an numerical aperture (NA) of 0.11. The pattern of a 200 m long fiber (fiber B) with a core diameter of 100 µm and an NA of 0.21 can be seen in Fig. 2B. Furthermore the speckle factor as a degree for the homogeneity of the beam profile was calculated using the following equation [10]:

$$F = \frac{H_{max}}{H_{mean}}, \tag{1}$$

where H_{max} is the maximum and H_{mean} the average radiant exposures. The ideal value which can only be achieved by a perfectly homogeneous top head beam profile is 1. With fiber A (standard coagulation fiber) a speckle factor of 2.9 could be obtained (radiant exposures distribution in Fig. 2A). This very high value has been lowered drastically by the application of fiber B to a value of 1.3 (Fig. 2B).

The coagulation laser is then superimposed with the pilot laser (HeNe 633 nm) imaged on the assay. The pilot laser (spot size = 500 µm) illuminates the smaller spot of the therapy laser (∼200 µm). The reflected light is captured via a 4f-system by a CCD camera 90 Hz (Prosilica, EC 655). The magnification achieved by the two lenses (f=100 mm and f=500 mm) is 5

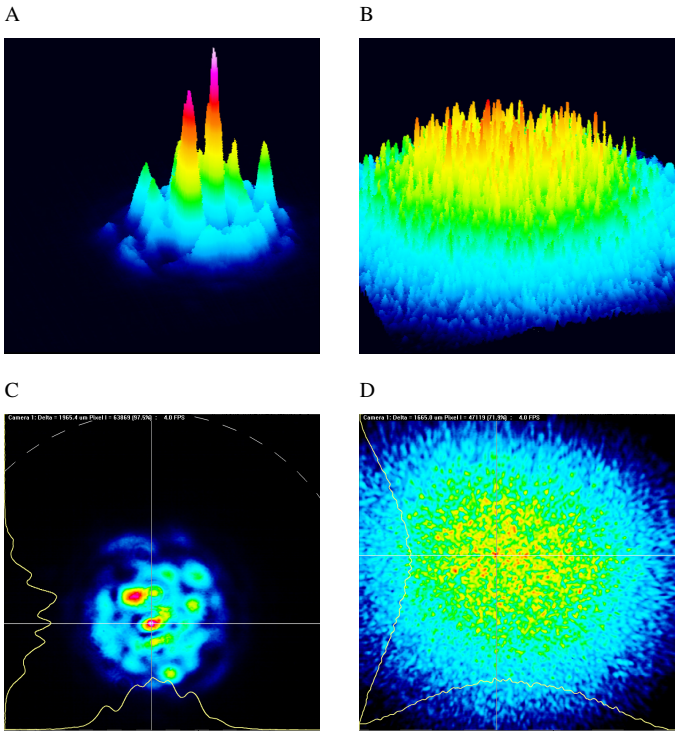

Fig. 2: 3D (top) and 2D (bottom) intensity distribution of the beam (532 nm); A/C: with a standard coagulation fiber and B/D: with a 200 m fiber. Superimposed on the 2D plot the intensity profile of the plane with the highest intensity in x and y direction is shown.

($M = f_2/f_1$).
The size of the speckle grains depend on the aperture of the optical system and is adjustable by the changeable iris.
To avoid brightness fluctuations during laser irradiation the heating laser light has been filtered by a notch filter for 532 nm (Semrock, StopLine®, Typical Notch Bandwidth = 17 nm). In order to synchronize the acquisition by the software with the laser pulse a photodiode is used as a trigger. A LabVIEW routine has been developed for all triggering, data collection and processing tasks.

C. Experiments on RPE-Phantoms and Porcine RPE

The speckle pattern is captured over 1 second with 47 frames per second (fps) to record 500 ms of heating during the laser pulse and 500 ms of relaxation subsequently. For initial experiments retina phantoms are used. They are made of silicon and consist of a black (silicon colour) lower part, representing the RPE where the major part of the light is absorbed, and a brighter grayish upper part typify the dispersive retina. Those models are used to optimize the optical setup, to get an first impression of the speckle movement and to improve the algorithms for the speckle estimation.
With the enhanced assembly tests on extracted pieces of porcine RPE with and without retina were performed. For this purpose strong pigmented pieces without vessels about 1x1 cm^2 were extracted from the pig eye, the vitreous was removed to reduce scattering. Besides several basic experiments for a better understanding of the speckle movement different heating

powers were tested to obtain a minimal detection sensitivity for the start of motion.

D. Motion Estimation and Speckle Tracking

In order to clarify and evaluate the speckle movement the velocity of the movement of brightness pattern (the optical flow), was calculated. The most common ways to recover the optical flow are based on spatial and temporal image derivations and can be classified in two methods, local and global ones. Here both methods are used. Global methods (Horn/Schunck) provide a dense flow field but are more sensitive to noise than local ones [11], [12]. Both are based on the same idea by Horn and Schunck that the brightness I (digitized voltage values from 0 to 255) of a particular point remains constant, at least for a short time [13]. They derived the optical flow constraint (OFC):

$$\frac{\partial I}{\partial x}\frac{dx}{dt} + \frac{\partial I}{\partial y}\frac{dy}{dt} + \frac{\partial I}{\partial t} = 0, \tag{2}$$

where $\frac{\partial I}{\partial x}$ and $\frac{\partial I}{\partial y}$ are the spatial and $\frac{\partial I}{\partial t}$ the temporal derivations of the brightness function at each image point and $\frac{dx}{dt}$ and $\frac{dy}{dt}$ the vertical and horizontal components of the velocity. At this point further constraints need to be introduced in order to uniquely determine the flow. Horn/Schunck established the smoothness constraints assuming that neighbored points have almost the same velocity and that the velocity of the brightness pattern varies smoothly to minimize the problem and to obtain the velocity iterative. In praxis horizontal and vertical velocity components are calculated for each pixel and superimposed to the current frame.
Lucas and Kanade on the other hand solved the flow equation for all points in a defined neighborhood by the method of least squares assuming that in that neighborhood the flow of all points is constant [14]. In this way the velocity of certain points can be calculated and thus the points can be tracked from frame to frame.

III. Results and Discussion

A. Experiments on Phantoms

The initial experiments in RPE-phantoms showed dynamic radial speckle movement away from the irradiation center during exposure and backwards after irradiation. The observed speckle could be characterized as translational speckle and not boiling speckle and therefore tracked using the Lucas Kanade algorithm which enabled the calculation of the moved distance of certain speckle for each frame. The mean value of 10 speckle is plotted over the time in Fig. 3 for different laser power applied on the same spot. For long exposure time (thermal equilibrium) the motion distance reached a maximum and the speckle pattern appeared static at the end of the pulse before the pattern moved back to original position.

B. Experiments on Porcine-RPE

The speckle movements observed on the porcine RPE with retina were similar to the speckle movements of the phantom. Both showed an speckle motion outwards during heating and towards the center afterwards. However, the speckle movement on porcine RPE without retina was different to those of the phantoms and the porcine RPE with retina. Instead of a motion outwards a movement towards the center of the heat source could be observed during heating and away from the center after heating accordingly.

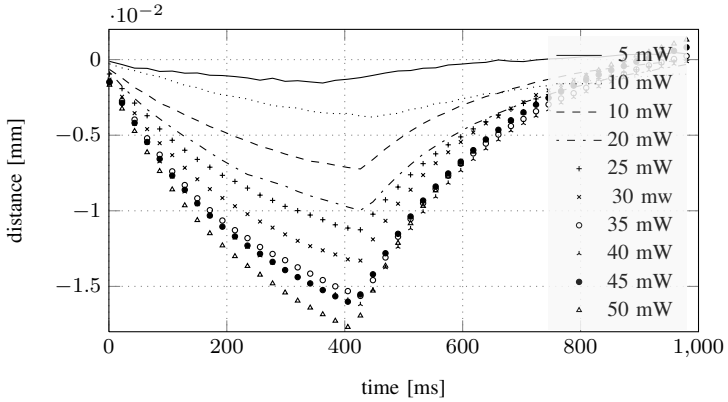

Fig. 3: Speckle movement (mean values over 10 speckle) during different laser power on the RPE phantom

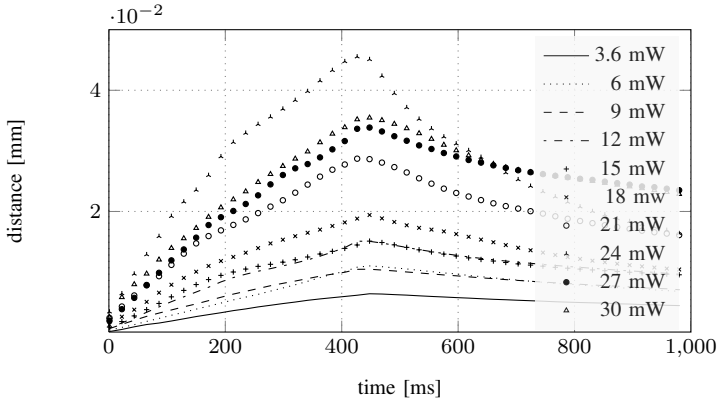

Fig. 4: Speckle movement (mean values over 20 speckle) during different power on porcine RPE without retina

In this context it has to be taken into consideration that the attachment of the retina to the RPE changes between in vivo to in vitro situations. In vitro (especially when the vitreous is removed) the retina will be detached from the RPE and its scattering properties are increasing. In vivo the retina is slightly attached to the RPE and is almost transparent. This leads to the assumption that with a loose retina the heated area gets larger due to scattering and leads to an expansion over the whole region and a lifting of the retina. Because the degree of detachment of the retina was unclear and hence its influence on the measurement the following result were achieved by using only the porcine RPE. Anyhow, the cause of the different movement on the RPE (speckle movement towards the center during heating) could not be clarified completely because no motion in z-direction was recorded. Furthermore is the influence of the different underlying structures not clear.
Fig. 4 shows the speckle movement (mean value over 20 speckle calculated using the Lucas Kanade algorithm) for different powers applied on the same spot and it is clear, that with rising power the movement is getting stronger. At

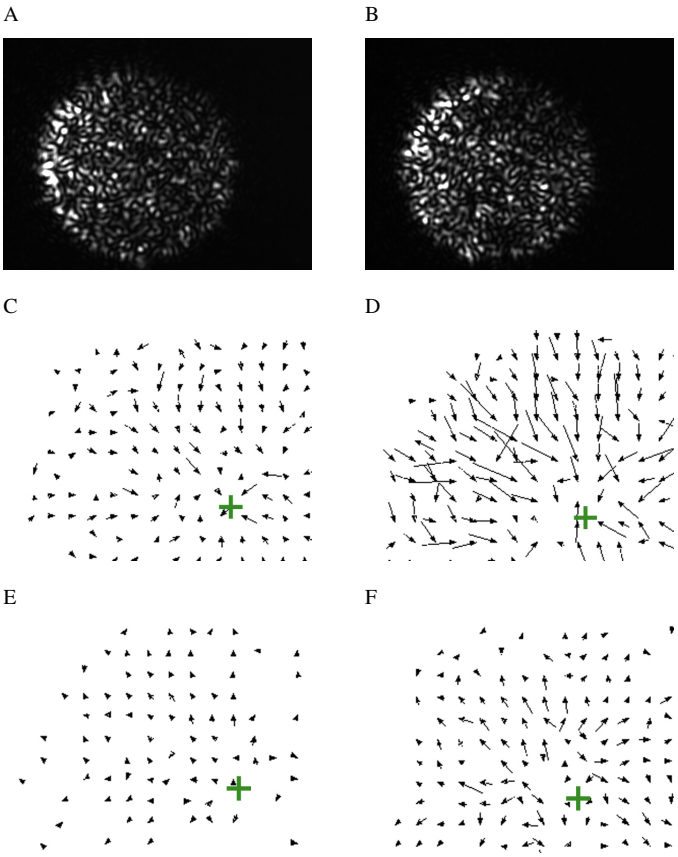

Fig. 5: Speckle pattern on porcine RPE without retina (A/B) and detail (upper left quadrant) of velocity vector maps during excitation, 213 ms (C/D) and relaxation, 638 ms (E/F); C/E: 6 mW, D/F: 30 mW. The + represents the heating spot center.

24 mW, there was a drastic increase of motion which leads to the assumption that a critical temperature threshold was reached and structural changes in the tissue were caused. But at this point no precise statement can be made because no simultaneous temperature measurement was performed. The relaxation movement which did not reach the original position after heating was not fully recorded. In organic tissue relaxation takes several seconds up to minutes.

In Fig. 5 speckle patterns (top) are shown as well as details from the velocity vector maps on the left side for 3.6 mW and on the right for 30 mW each during coagulation, 213 ms (middle) and relaxation, 638 ms (bottom). For both powers the vectors pointing towards the spot center which represents a movement of the tissue in the same direction. After the pulse the vectors change their direction and the tissue is moving back. The lengths of the vectors show that the velocity is stronger during excitation (Fig. 5D) than relaxation (Fig. 5F) which confirm the statement that relaxation of the tissue to an original position takes much longer than the excitation owing to longer cooling time since heating is not in the time of thermal equilibrium. While at 3.6 mW there is only movement in the spot center at 30 mW there are larger vectors over the whole image which mean that also the tissue outside the therapy laser spot thus a much larger area is moving due to heat diffusion.

IV. Conclusions

In this project speckle movements have been studied during photocoagulation of extracted porcine RPE with and without retina and RPE like phantoms. It has been found that the dynamic speckle behavior can be categorized as translational speckles and therefore they can be tracked over time. The movements of those speckle correspond to the tissue movements. Further analyses have shown that the velocity of the movement, the distance and the area in which movement occurs increase with the irradiance. The origin of the movement could not be clarified for now because the sum of the thermal movements of RPE, Bruchs Membrane, Choroidea and Sklera has been measured. According to the findings it may be possible to calculate a mean temperature correlated value (comparable to optoacoustics [7]) which offers the possibility of designing a dosimetry system based on laser speckle analysis. In the next months this new concept will be applied together with the existing optoacoustic technique on RPE cells to correlate the speckle movements to simultaneous measured temperatures. Furthermore the design of an algorithm which is able to correct global movements of the treated object is necessary.

References

[1] A.M. Shah, N.M. Bressler, and L.M. Jampol. Does laser still have a role in the management of retinal vascular and neovascular diseases? *American journal of ophthalmology*, 152(3):332–339, 2011.

[2] Early Treatment Diabetic Retinopathy Study research group. Photocoagulation for diabetic macular edema. Early Treatment Diabetic Retinopathy Study report number 1. *Arch. Ophthalmol.*, 103(12):1796–1806, 1985.

[3] Branch Vein Occlusion Study Group. Argon laser scatter photocoagulation for prevention of neovascularization and vitreous hemorrhage in branch vein occlusion. A randomized clinical trial. *Arch. Ophthalmol.*, 104(1):34–41, 1986.

[4] The Central Vein Occlusion Study Group. Natural history and clinical management of central retinal vein occlusion. *Arch. Ophthalmol*, 115(4):486–491, 1997.

[5] S.Y. Schmidt and R.D. Peisch. Melanin concentration in normal human retinal pigment epithelium. regional variation and age-related reduction. *Investigative ophthalmology & visual science*, 27(7):1063–1067, 1986.

[6] W.J. Geeraets, RC Williams, G. Chan, W.T. Ham Jr, D. GUERRY III, and F.H. Schmidt. The relative absorption of thermal energy in retina and choroid. *Investigative Ophthalmology & Visual Science*, 1(3):340–347, 1962.

[7] R. Brinkmann, S. Koinzer, K. Schlott, L. Ptaszynski, M. Bever, A. Baade, S. Luft, Y. Miura, J. Roider, and R. Birngruber. Real-time temperature determination during retinal photocoagulation on patients. *Journal of Biomedical Optics*, 17(6):061219–1, 2012.

[8] K. Schlott, S. Koinzer, L. Ptaszynski, M. Bever, A. Baade, J. Roider, R. Birngruber, and R. Brinkmann. Automatic temperature controlled retinal photocoagulation. *Journal of Biomedical Optics*, 17(6):061223–1, 2012.

[9] H.J. Rabal and R.A. Braga Jr. *Dynamic laser speckle and applications*, volume 139. CRC, ISBN-13: 978-1-4200-6015-7, 2008.

[10] W. Lauterborn, T. Kurz, and M. Wiesenfeldt. *Kohärente Optik: Grundlagen für Physiker und Ingenieure; mit 73 Aufgaben und vollständigen Lösungen*. Springer, 1993.

[11] J.L. Barron, D.J. Fleet, and SS Beauchemin. Performance of optical flow techniques. *International journal of computer vision*, 12(1):43–77, 1994.

[12] B. Galvin, B. McCane, K. Novins, D. Mason, S. Mills, et al. Recovering motion fields: An evaluation of eight optical flow algorithms. In *British Machine Vision Conference*, volume 1, pages 195–204, 1998.

[13] B.K.P. Horn and B.G. Schunck. Determining optical flow. *Artificial intelligence*, 17(1):185–203, 1981.

[14] B.D. Lucas, T. Kanade, et al. An iterative image registration technique with an application to stereo vision. In *Proceedings of the 7th international joint conference on Artificial intelligence*, pages 674–679, 1981.